

The formation of the neutrino-driven wind termination shock in 1D core collapse SN models using Boltzmann neutrino transport

T. Fischer*, C. Winteler†, U. Frischknecht, F.-K. Thielemann and M. Liebendörfer

Department of Physics, University of Basel, Klingelbergstrasse 82, 4056 Basel, Switzerland

The recent implementation of a nuclear reaction network into our core collapse model, makes it possible to investigate the post bounce evolution for several *seconds*. The network is relevant for temperatures below 0.5 MeV to accurately calculate the binding energy contribution to the internal energy.

Since the explosion mechanism is yet a subject of debate, we artificially enhance the neutrino heating and cooling rates to trigger an explosion in general relativistic spherically symmetric core collapse simulations using three flavour Boltzmann neutrino transport. After the explosion has been launched, a region of low density and high entropy forms between the explosion shock and the protoneutron star (PNS) at the center. There, neutrino heated material is accelerated from the PNS surface, known as the neutrino wind. This material is decelerated behind the explosion shock. The low temperatures in that region favor the freeze out of light nuclei, which is modeled using our nuclear reaction network.

We will discuss the possibility of the formation of the supersonic neutrino wind as well as the formation of a shock, the neutrino-driven wind termination shock, for different low and intermediate mass progenitor models during the post bounce phase.

*10th Symposium on Nuclei in the Cosmos
July 27 - August 1 2008
Mackinac Island, Michigan, USA*

*This work has been supported by the Swiss National Science Foundation, grand no. PP002-106627/1

†Speaker.

1. Core collapse supernovae in spherical symmetry

Our model is based on an implicit three-flavour Boltzmann neutrino transport solver in spherical symmetry [1] describing the neutrino transport as well as microphysical interactions between neutrinos and the fluid [2, 3, 4]. In order to treat the post-bounce phase, this Lagrangian model was coupled to an implicit general relativistic code that features an adaptive grid [5]. Special emphasis has been given to implement a finite differencing of the coupled transport and hydrodynamics equations, that accurately conserves lepton number and energy in the post-bounce phase [6]. To be able to handle nuclear abundances in the regime of temperatures below 0.5 MeV, a nuclear reaction network has been included recently [7]. For higher matter temperatures, an equation of state (EoS) for hot and dense nuclear matter is used [8].

Despite the lack of explosions using spherically symmetric core collapse models for progenitors more massive than $8 M_{\odot}$ [9, 10, 11], by increasing the reaction rates for the electronic charged current reactions artificially, we are able to investigate neutrino-driven explosions [12, 13]. This leads to weak explosions with explosion energies of $\simeq 1 - 5 \times 10^{50}$ erg. Such explosion models have been investigated with respect to the nucleosynthesis in general [15] and induced by the νp -process [16].

2. The neutrino wind phase

After the explosion has been launched at about 500 ms after bounce (depending on the progenitor model and the explosion parameter), the expanding explosion shock propagates into the region where nuclear reactions (Si and O burning) dominate the internal energy evolution. The protoneutron star (PNS) at the center, identified at the neutrinospheres in Fig. 1 (a), settles down to a quasi-stationary state and contracts on timescales of seconds. The neutrinos emitted at the neutrinosphere heat the surface of the PNS. The heated material is accelerated to positive velocities, as shown in Fig. 1 (a). This phenomenon is known as the neutrino-driven wind [17], [18].

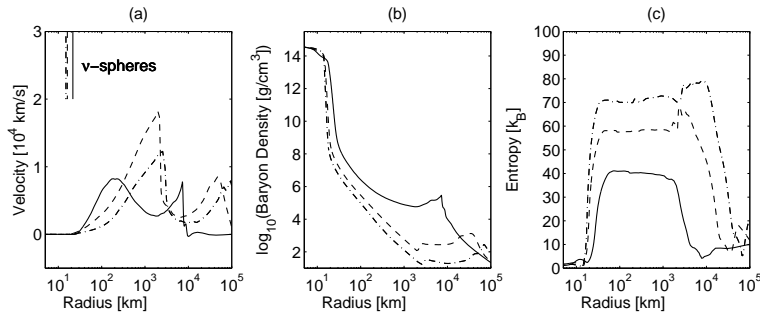


Figure 1: Radial velocity, density and entropy profiles during the post bounce evolution of a $10 M_{\odot}$ progenitor model [21] at 1 s (solid lines), 5 s (dashed lines) and 10 s (dash-dotted lines) after bounce.

The neutrino wind develops supersonic velocities, here already 3.6 s after bounce for the $10 M_{\odot}$ progenitor model under investigation, which is in qualitative agreement with ref. [19]. This produces a second shock, the wind termination shock (see Fig. 1 (a) and (b)). However, the accelerated material does not overcome the density jump of the explosion shock. Matter is

decelerated and deposit behind the explosion shock, as illustrated in Fig. 2 (b). Hence, the matter velocities reduce again as shown in Fig. 1 (a) at about 10 s after bounce.

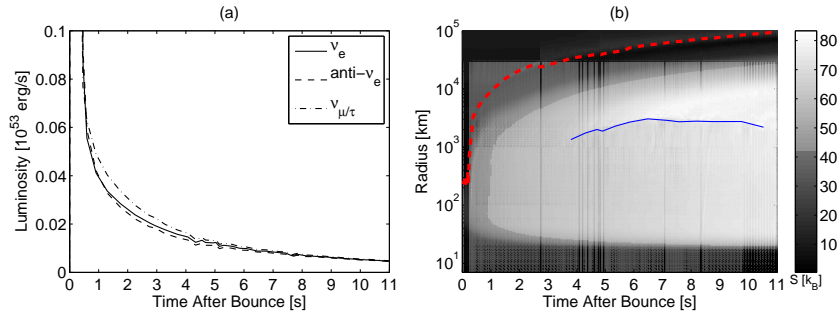


Figure 2: Luminosities and mass shells as a function of time after bounce, with the gray-scaled entropy per baryon. The red dashed line shows the position of the explosion shock and the blue solid line the position of the wind termination shock.

Between the neutrinospheres and the expanding explosion shock, the neutrino wind results in high entropies. While the initial neutrino-driven wind proceeds almost adiabatically, the entropy of the wind termination shock reaches several $\simeq 80 k_B/n_B$, as illustrated in Fig. 1 (c) about 10 s after bounce. In the following dynamical evolution, the wind entropy continues to increase and reaches above $100 k_B/n_B$. On the other hand, the matter density and temperature of the neutrino wind region decrease rapidly, as illustrated in Fig. 1 (b). There, a nuclear reaction network becomes necessary to model the dynamically changing composition accurately, especially the decreasing number of free nucleons due to the freeze out of nuclei (α -rich freeze out). This is important for the binding energy contribution to the internal energy and the weak interaction rates, which depend on the number density of free nucleons. About 15 s after bounce, the contracting PNS has a radius of about 15 km (see Fig. 2) and a central matter density of $\rho \simeq 4 \times 10^{14}$ g/cm³ (for the $10 M_\odot$ progenitor model under investigation).

As soon as neutrino heating (for the ν -reactions used, see [14] and ref. in there) deposits enough energy behind the standing accretion shock to launch the explosion on timescales of 100 ms, the neutrino luminosities decrease exponentially. Due to the low luminosities of $\simeq 10^{50}$ erg/s, (see Fig. 2) the matter velocities of the wind termination shock become sub-sonic again. Finally, the termination shock vanishes and the neutrino wind settles down to a quasi-stationary state about 25 s after bounce for the $10 M_\odot$ progenitor model under investigation, while the explosion shock continues to expand.

3. Discussion

Because these results depend strongly on the progenitor model, we analyzed the 10 and the $15 M_\odot$ progenitor model [21] during the explosion phase (via artificially enhanced neutrino heating rates) into the neutrino wind phase. With these increased reaction rates, the neutrino-driven wind does always develop for both progenitor models under investigation. However, only for the $10 M_\odot$ progenitor model the wind becomes supersonic and develops into the neutrino-driven wind termination shock. The more compact $15 M_\odot$ progenitor model (see Fig. 3 (b)) prevents the matter

velocities from becoming supersonic. The wind termination shock remains absent, as illustrated in Fig. 3 (a).

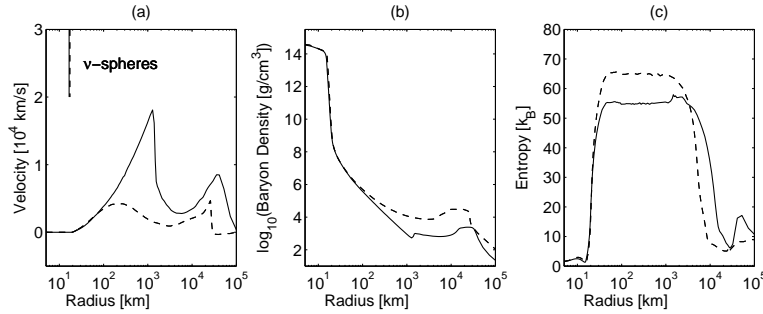


Figure 3: The same configuration as Fig. 1, comparing the two progenitor models under investigation ($10 M_{\odot}$: solid lines, $15 M_{\odot}$: dashed lines) during the neutrino wind phase at the maximum wind (termination shock) velocities about 4 s after bounce.

In addition, if we switch back to the standard neutrino reaction rates [3] after the explosion shock has been launched, the neutrino wind remains sub-sonic for all times after bounce and does not develop to a shock for either of the progenitor models under investigation.

4. Outlook

The formation of the neutrino-driven wind termination shock and the impact of the neutrino wind to nucleosynthesis calculations is a subject of research. The large entropies have been suggested as a possible site for the r -process. However, we find that the small amount of mass that accompanies the neutrino wind and the rapidly decreasing density might lead to less favourable conditions for the r -process, as discussed in ref. [20] for the $8 M_{\odot}$ O-Ne-Mg core from ref. [9, 10].

At 30 s after bounce, the quasi-static PNS has already entered the early neutrino dominated cooling phase, identified as the maximal matter temperature inside the PNS decreases from initially $\simeq 30$ MeV at $\simeq 500$ ms after bounce to < 10 MeV at $\simeq 25$ s after bounce. The PNS is still in an accreting environment (fall back of mass inside the mass cut), neutrinos are treated using Boltzmann neutrino transport and the freeze out of nuclei at the PNS surface (forming the neutron star crust and envelop) is modeled using a nuclear reaction network, all of which is beyond present quasi-hydrostatic neutron star cooling models (see for example [22, 23, 24]).

References

- [1] A. Mezzacappa and S. W. Bruenn. *ApJ*, 405:637–668, March 1993, *ApJ*, 405:669–684, March 1993, *ApJ*, 410:740–760, March 1993.
- [2] P. J. Schinder and S. L. Shapiro. *ApJS*, 50:23–37, September 1982.
- [3] S. W. Bruenn. *ApJS*, 58:771–841, August 1985.

- [4] A. Mezzacappa and O. E. B. Messer. *Journal of Computational and Applied Mathematics*, 109:281–319, September 1999.
- [5] M. Liebendörfer, A. Mezzacappa, and F.-K. Thielemann. *PRD*, 63(10):104003–+, May 2001.
- [6] M. Liebendörfer, O. E. B. Messer, A. Mezzacappa, S. W. Bruenn, C. Y. Cardall, and F.-K. Thielemann. *ApJS*, 150:263–316, jan 2004.
- [7] F.-K. Thielemann, F. Brachwitz, P. Höflich, G. Martínez-Pinedo, and K. Nomoto. *New Astronomy Review*, 48:605–610, May 2004.
- [8] H. Shen, H. Toki, K. Oyamatsu, and K. Sumiyoshi. *Progress of Theoretical Physics*, 100: 1013–1031, November 1998.
- [9] K. Nomoto. *ApJ*, 277:791–805, February 1984.
- [10] K. Nomoto. *ApJ*, 322:206–214, November 1987.
- [11] F. S. Kitaura, H.-T. Janka, and W. Hillebrandt. *A&A*, 450:345–350, April 2006.
- [12] H. A. Bethe and J. R. Wilson. *ApJ*, 295:14–23, August 1985.
- [13] A. Mezzacappa, J. M. Blondin, O. E. B. Messer, and S. W. Bruenn. In *Origin of Matter and Evolution of Galaxies*, volume 847 of *American Institute of Physics Conference Series*, pages 179–189, July 2006.
- [14] T. Fischer, S. C. Whitehouse, A. Mezzacappa, F. K. Thielemann and M. Liebendörfer. eprint = arXiv:astro-ph/0809.5129v1
- [15] C. Fröhlich, P. Hauser, M. Liebendörfer, G. Martínez-Pinedo, F.-K. Thielemann, E. Bravo, N. T. Zinner, W. R. Hix, K. Langanke, A. Mezzacappa, and K. Nomoto. *ApJ*, 637:415–426, January 2006.
- [16] C. Fröhlich, G. Martínez-Pinedo, M. Liebendörfer, F.-K. Thielemann, E. Bravo, W. R. Hix, K. Langanke, and N. T. Zinner. *PRL*, 96(14):142502–+, April 2006.
- [17] R. C. Duncan, S. L. Shapiro and I. Wassermann. *ApJ* **309**, 141, 1986.
- [18] S. E. Woosley and E. Baron. *ApJ* **391**, 228, 1992.
- [19] A. Arcones, H.-T. Janka, and L. Scheck. *A&A*, 467:1227–1248, June 2007.
- [20] H.-T. Janka, B. Müller, F. S. Kitaura, and R. Buras. *A&A*, 485:199–208, July 2008.
- [21] S. E. Woosley, A. Heger, and T. A. Weaver. *Reviews of Modern Physics*, 74:1015–1071, nov 2002.
- [22] D. Page. *ApJ*, 442:273–285, March 1995.
- [23] J. A. Pons, F. M. Walter, J. M. Lattimer, M. Prakash, R. Neuhäuser, and P. An. *ApJ*, 564: 981–1006, January 2002.
- [24] J. A. Henderson and D. Page. *APSS*, 308:513–517, April 2007.